

Human induced pluripotent stem cells derived endothelial cells mimicking vascular inflammatory response under flow

Li Wang,^{1,2} Meng Xiang,¹ Yingying Liu,¹ Ning Sun,¹ Meng Lu,¹ Yang Shi,² Xinhong Wang,¹ Dan Meng,¹ Sifeng Chen,^{1,a)} and Jianhua Qin^{2,a)}

¹Department of Physiology and Pathophysiology, College of Basic Medical Sciences, Fudan University, Shanghai 200032, People's Republic of China

²Dalian Institute of Chemical Physics, Chinese Academy of Sciences, Dalian 116023, People's Republic of China

(Received 17 November 2015; accepted 5 January 2016; published online 13 January 2016)

Endothelial cells (ECs) have great potential in vascular diseases research and regenerative medicine. Autologous human ECs are difficult to acquire in sufficient numbers *in vitro*, and human induced pluripotent stem cells (iPSCs) offer unique opportunity to generate ECs for these purposes. In this work, we present a new and efficient method to simply differentiate human iPSCs into functional ECs, which can respond to physiological level of flow and inflammatory stimulation on a fabricated microdevice. The endothelial-like cells were differentiated from human iPSCs within only one week, according to the inducing development principle. The expression of endothelial progenitor and endothelial marker genes (GATA2, RUNX1, CD34, and CD31) increased on the second and fourth days after the initial inducing process. The differentiated ECs exhibited strong expression of cells-specific markers (CD31 and von Willebrand factor antibody), similar to that present in human umbilical vein endothelial cells. In addition, the hiPSC derived ECs were able to form tubular structure and respond to vascular-like flow generated on a microdevice. Furthermore, the human induced pluripotent stem cell-endothelial cells (hiPSC-ECs) pretreated with tumor necrosis factor (TNF- α) were susceptible to adhesion to human monocyte line U937 under flow condition, indicating the feasibility of this hiPSCs derived microsystem for mimicking the inflammatory response of endothelial cells under physiological and pathological process. © 2016 AIP Publishing LLC. [<http://dx.doi.org/10.1063/1.4940041>]

I. INTRODUCTION

The vascular system is crucial to the maintenance of tissue homeostasis and the repair of damaged tissues in adults.¹ Defects in the vascular system can result in many kinds of vascular-related disease, including diabetic retinopathy, myocardial ischemia, and atherosclerosis.²⁻⁴ Endothelial cells (ECs) form the lining of blood vessels and play a crucial role in maintaining their integrity and normal function in vascular regeneration and tissue engineering applications. Damage to the endothelium occurs at an early stage in most vascular diseases. However, human-derived ECs are difficult to acquire for injury treatment and tissue engineering; thus, it is highly desirable to develop a suitable method for obtaining abundant human ECs *in vitro*.

Induced pluripotent stem cells (iPSCs) were originally generated from mouse somatic fibroblasts transfected with retroviruses containing Oct3/4, Sox2, c-Myc, and Klf4.⁵ A year later, Yamanaka and Thomson independently constructed human iPSCs from human dermal fibroblasts using a virus containing transcriptional regulators of pluripotency.^{6,7} Due to their capacity for long-term self-renewal and multipotent differentiation, human iPSCs are highly promising cell sources for a wide range of biomedical applications, including disease mechanism research,

^{a)}Authors to whom correspondence should be addressed. Electronic addresses: chen1216@fudan.edu.cn, Telephone/Fax: 011-86-21-54237623 and jhqin@dicp.ac.cn, Telephone: 86-411-84379650, Fax: 86-411-84379059.

tissue/organ engineering, cellular replacement therapies, and pharmacology and toxicology screening.^{8–10} The capacity of hiPSCs to differentiate into particular cellular lineages is undergoing intensive study. Recently, hiPSCs have been differentiated into cardiomyocytes, pancreatic β -like cells, endothelial cells, and other cell types.^{11–13} ECs derived from hiPSCs have great potential as a source for vascular regeneration and tissue engineering.

The most common method for differentiation is based on the strategy of differentiating embryonic stem cells (ESCs) by generating embryoid bodies (EBs). ECs derived from iPSCs are about between 5% and 20% using EBs method.¹³ The efficiency is too low to meet the demands of clinical treatment and tissue engineering. Kane *et al.* reported a two-dimensional directed differentiation protocol for obtaining ECs from human embryonic stem cells (hESCs). Despite an increase in efficiency, the differentiation time was up to 21 days.¹⁴ Zhang differentiated hiPSCs into endothelial cells using a three-dimensional fibrin scaffold.¹⁵ The differentiation efficiency was up to 45%, but the differentiation time was more than two weeks. Currently, several strategies are available to obtain ECs from iPSCs, such as differentiating hiPSCs into angioblasts or endothelial-hematopoietic progenitor cells by magnetic-activated cell sorting (MACS) or flow cytometry. However, these methods largely depend on special antibody and external instruments, and it is also easier to get contamination during the multi-step of sorting process.

In this work, we describe a new and straightforward approach for differentiating human derived iPSCs into functional ECs with high efficiency and less time. We mixed bone morphogenic protein 4 (BMP4), activin A, basic fibroblastic growth factor (bFGF-2), and vascular endothelial growth factor (VEGF) in the first differentiation stage. These factors mediate the commitment of mesoderm to differentiate into cardiovascular cells.^{16–20} The rho-associated protein kinase (ROCK) inhibitor, Y27632, and a selective inhibitor of the transforming growth factor- β (TGF- β) receptor, SB431542, have been reported to promote endothelial cell proliferation and survival.^{21–23} The differentiated endothelial-like cells could be obtained within only one week. The purity reached 60% after manual purification. The differentiated ECs exhibited the capability to form capillary structure and demonstrated strong expression of EC-specific markers. Moreover, the ECs can respond to a physiological level of flow on a microfluidic device, analogous to dynamic vascular microenvironment *in vivo*. Furthermore, the hiPSC-ECs pretreated with TNF- α were susceptible to adhesion to human monocyte under flow condition, suggesting the utility of this hiPSC-derived microsystem for mimicking the inflammatory response of endothelial cells in pathogenesis.

II. MATERIALS AND METHODS

A. Cell culture and characterization

Human iPSCs were kindly provided by Professor Ning Sun (Fudan University, China). These cells were prepared and characterized as described previously.²⁴ Cells were cultured on dishes coated with Matrigel diluted at 60:1 (BD Bioscience) in mTeSR1 medium (STEMCELL Technologies, Canada). To characterize hiPSCs, we performed alkaline phosphatase (AP) assays (Beyotime Institute of Biotechnology) and immunofluorescence assays using antibodies against the pluripotency markers octamer-binding transcription factor 4 (OCT4, Cell Signaling Technology, USA) and SRY (sex determining region Y)-box 2 (SOX2, Cell Signaling Technology, USA). The AP assay was performed according to the manufacturer's manual. The detailed immunofluorescence process was as described below.

Human umbilical vascular epithelial cells (HUVECs) were cultured in a specific endothelial cell medium (ECM, ScienCell Company, USA) containing 100 units ml^{-1} penicillin and 100 units ml^{-1} streptomycin. Human monocytic tumor cell line U937 was cultured in 1640 medium containing 10% fetal bovine serum (FBS, Gibco, USA), 100 units ml^{-1} penicillin and 100 units ml^{-1} streptomycin (Invitrogen, USA). We identified the HUVEC using CD31 (Cell Signaling Technology, USA) and the von Willebrand factor antibody (vWF) (Santa Cruz Biotech, USA) by immunofluorescence assay.

B. Fabrication of microfluidic device

To investigate the interaction between hiPSC-derived ECs and monocytes *in vitro*, we developed a microfluidic chip with microchannels to mimic vessels *in vivo*. A schematic of the chip is shown in Fig. 5. The microdevice has three parts: a glass substrate layer, a layer of polydimethylsiloxane (PDMS, Sylgard 184, Dow Corning) with channels, and a perfusion system. The device was fabricated using standard photolithographic technology.²⁵ Briefly, we developed an SU8-3035 (Microchem, Newton, MA, USA) mold with two channels and replicated a PDMS layer with microchannels (length \times width \times depth: 10 mm \times 400 μ m \times 200 μ m) by thoroughly mixing the PDMS base with a curing agent (10:1 by mass). The polymer was cured in an oven for 40 min at 80 °C. The PDMS layer was then gently peeled away from the mold, and inlet and outlet holes were made with a razor-sharp punch. Finally, the PDMS layer was irreversibly bonded onto a clean glass wafer with oxygen plasma for 45 s. The chip was sterilized with UV light for 30 min, and the microchannels were coated with 50 μ g/ml collagen I (Corning Inc., USA). Collagen I was used to promote the ECs to attach to the PDMS substrate. The channels were washed with phosphate-buffered saline (PBS) prior to culturing the cells.

C. Strategy of differentiating hiPSC into ECs

We established a two-step, two-dimensional, and direct differentiation method without hiPSCs proliferation using a mixture of BMP4 (Invitrogen Tech.), activin A (Invitrogen Tech.), VEGF (Invitrogen Tech.), bFGF (Invitrogen Tech.), Y27632 (Selleckchem Tech.), and SB431542 (Selleckchem Tech.). Briefly, 10–15 clones/cm² of hiPSCs with approximately 10–50 cells per clone were cultured on the original concentration of Matrigel according to the manufacturer's instructions. In stage 1, the cells were cultured in DMEM-F12 medium containing 3% FBS, 50 ng/ml BMP4, 10 ng/ml activin A, 50 ng/ml VEGF, and 50 ng/ml bFGF for 1 day. In stage 2, the medium was changed to ECM supplemented with 50 ng/ml VEGF, 50 ng/ml bFGF, 10 μ M Y27632, and 10 μ M SB431542, and the cells were cultured for 2 to 7 days. The cells were subcultured on a dish coated with Matrigel (diluted 1:60) in ECM and were expanded when the cells were >90% confluent. Images of the cells were recorded each day. We designated the cells cultured in differentiating medium as passage 0 (P0), the first subculture in ECM as passage 1 (P1), and subsequent passages were numbered accordingly.

D. RNA isolation and reverse transcription—Real time quantitative polymerase chain reaction

We analyzed the genes expression related with vascular system development to clarify the mechanism of hiPSCs differentiating into ECs in present study. The total RNA of the cells was extracted using TRIzol reagent on days 2, 4, and 6. Briefly, the cells were washed with ice cold PBS three times then the PBS was removed as far as possible, and 0.125 ml/cm² TRIzol was added for 5 min at room temperature (RT). The TRIzol/cell lysate was transferred to a 1.5 ml Eppendorf tube. Chloroform was added to the lysate in a 1:4 ratio of TRIzol to chloroform. The mixture was shaken vigorously for about 15 s and left at RT for 5 min. After centrifuging at 10 000 rpm for 10 min, the aqueous phase was carefully removed using a pipette. The supernatant was mixed with an equal volume of isopropanol at RT for 20 min, and the mixture was then centrifuged at 10 000 rpm for 15 min. RNA was visible as a deposit at the bottom of the tube. The isopropanol was poured off and 1 ml 75% ethanol in DEPC (Diethylpyrocarbonate) treated ddH₂O was added. The samples were recentrifuged at 7500 rpm for 10 min then the ethanol was poured off and the pellets air-dried. The RNA was then dissolved with 15–20 μ l DEPC treated ddH₂O.

RNA (2 μ g) was reverse-transcribed using random-sequence primers with a PrimeScript 1st Strand cDNA Synthesis Kit. The relative levels of gene expression were determined using quantitative PCR (qPCR) with an SYBR PrimeScript RT reagent kit. The pluripotency marker gene (SOX2), a specific marker of mesoderm (brachyury), transcription factors GATA2 and RUNX1, which regulate the development of the hemogenic endothelium, markers of endothelial

progenitor cells and mature ECs, vascular endothelial-cadherin (VE-cadherin) CD31, and CD34, and the hematopoietic marker stem cell leukemia (SCL) gene were tested. The levels of all transcripts were normalized to those of β -actin mRNA. The data were analyzed using the $2^{-\Delta Ct}$ method. All samples were analyzed in triplicate from independent assays. We identified the hiPSC as induced pluripotent stem (IPS), and hiPSC-derived endothelial cells as I-E(n), where “n” represents the number of days of differentiation into ECs. All reagents were purchased from Takara Technology (Japan). The primer sequences are shown in the supplementary Table.³⁷

E. Immunofluorescence analysis

To characterize the hiPSCs, hiPSC-derived ECs, and HUVECs, we performed immunofluorescence assays. Briefly, the cells were cultured on 24 well plates for 48 h. The cells were washed with cold PBS then fixed with 4% (w/v) paraformaldehyde in PBS for 10 min at RT. The cells were then permeabilized with 0.2% (v/v) Triton-100 (Sigma, USA) in PBS for 10 min at RT and then washed with PBS three times. To avoid non-specific binding of the antibodies, the cells were incubated with normal goat serum (Beyotime Company, China) at RT for 45–60 min. The cells were then incubated with primary antibodies, SOX2 and OCT4 for hiPSCs (diluted 1:300, Cell Signaling Technology, USA), CD31 (diluted 1:300, Cell Signaling Technology, USA), and vWF (diluted 1:100, Santa Cruz Biotech, USA) for hiPSC-derived ECs and HUVECs at 4 °C overnight. Alexa 594 or 488 conjugated goat secondary antibodies (diluted 1:100, Beyotime Company, China) in PBS were added to the cells for 60 min at RT in the dark, after which the samples were washed three times with PBS for 5 min. The nuclei were counterstained with 40,6-diamidino-2-phenylindole (DAPI, Sigma) for 5 min at RT in the dark. All images were acquired using a photomicrograph or fluorescence microscope (Leica).

F. *In vitro* tube formation assay

To investigate the function of the hiPSC-ECs, we performed a tube formation *in vitro* as previously described.²⁶ Following the manufacturer’s instructions, the thin gel method was used for plating the ECs on top of the gel. Briefly, Matrigel (354234, Corning Inc., USA) was thoroughly thawed at 4 °C. After mixing the Matrigel using cooled pipets on ice, we added 50 $\mu\text{l}/\text{cm}^2$ to the growth surface in 24 well plates that were placed on ice. The plates were incubated at 37 °C for 30 min to solidify the Matrigel. The second-generation ECs differentiated from hiPSCs and same passage of HUVECs were trypsinized and seeded onto solidified Matrigel at a density of 1×10^5 per well for 24 h. Capillary-like structures were photographed using a phase-contrast microscope (Leica), and the numbers of intact tubes and branches per knot were counted and analyzed.

G. Purification of hiPSC-derived ECs and flow cytometric analysis

To determine the efficiency of differentiation, we identify the purification of ECs from hiPSCs using CD31 protein marker by flow cytometry. Human iPSC-derived ECs were trypsinized and subcultured on six-well plates coated with Matrigel (diluted 1:60). The centers of the cellular masses were not ECs according to their morphology, and they were removed by manual scraping. P1 or purified P2 endothelial-like cells derived from hiPSCs were harvested using a solution of 0.2% trypsin/EDTA for 3–5 min at RT. The cells were incubated for 1 h at RT with antibodies against human CD31 (Santa cruze, diluted 1:150) after blocking in PBS/1% bovine serum albumin. After washing three times with PBS, the cells were incubated with fluorescein isothiocyanate (FITC)-conjugated secondary antibodies for 45 min at RT. Incubation with the corresponding IgG isotype served as the negative control. The data were analyzed using a FACS Calibur (BD Biosciences).

H. Human iPSC-derived ECs responding to flow stress

To investigate the response of hiPSC-ECs to flow stress, we used a microfluidic chip with microchannels to mimic vessels *in vivo*. The hiPSC-ECs of passage 3 were trypsinized and

purified via MACS using CD31 magnetic antibodies (Miltenyi Biotech) according to the manufacturer's instructions. The purified hiPSC-derived ECs were resuspended at a density of 1×10^7 cells/ml and perfused into the microchannels. The cells were allowed to attach for 12 h prior to flow. The chamber flow shear stress was estimated to be 10 dyn/cm^2 , flow rate is $228 \text{ } \mu\text{l/min}$, which is similar to physiological flow rate present in microvessels,^{27–29} using the formula $\tau = 6\mu Q/wh^2$, where μ is the viscosity of the medium, Q is the flow rate, and w and h are width and height of the chamber, respectively.^{30–32} The hiPSC-derived ECs were perfused with normal medium for 24 h. The cellular arrangement was evaluated according to the angle between the cellular long axis and the flow direction. The number of cells within same angle area in unit circle area was counted according to the cell arrangement. In this study, the angular range was divided as -30° to $+30^\circ$, 30° to 60° / -30° to -60° , 60° to 90° / -60° to -90° . The cells cultured in static condition were used as a control.

I. Effects of inflammatory stimulation on human iPSC-derived ECs under flow

To evaluate the response of human iPSC-derived ECs to inflammatory stimulation under flow condition, we developed an inflammatory model using microdevices. Briefly, hiPSC-derived ECs at a density of 1×10^7 cells/ml were seeded into the channels for 12 h prior to flow. The confluent cells were perfused with normal medium containing 25 ng/ml TNF- α for 4 h under low flow at 1 dyn/cm^2 . Normal medium without TNF- α was the control. U937 cells at density of 5×10^5 cells/ml were perfused into the endothelial channels at $50 \text{ } \mu\text{l/min}$ for 30 min after stained with live cell dye PKH26 (Sigma, USA). The non-adhered cells were washed with normal medium after static culture for 15 min. All samples were fixed with 4% (w/v) paraformaldehyde for the immunofluorescence assays. The tight junctions among the ECs were tested by immunofluorescence using ZO-1 antibodies (diluted 1:100, Santa Cruz Biotech, USA). The adhesive U937 cells were counted in five random fields under a $400\times$ microscope. All experiments were completed in triplicate.

III. STATISTICAL ANALYSIS

Data, which are expressed as the means \pm standard deviation, were analyzed using one-way analysis of variance or the Student's *t*-test. Statistical significance was defined as $P < 0.05$.

IV. RESULTS AND DISCUSSION

A. Characterization of hiPSCs and differentiation scheme of hiPSCs into ECs

In this work, the hiPSCs derived from human dermal fibroblast were constructed by Professor Ning Sun (Fudan university). As it is important to maintain the pluripotent property of hiPSCs before they can be differentiated into other specific cells, we initially identified the undifferentiated features of hiPSCs. Immunofluorescence analyses showed that the cells expressed SOX2 and OCT4 in the nucleus and expressed alkaline phosphatase in the cytoplasm (supplementary Figure A).³⁷ These results demonstrate that hiPSCs maintained good pluripotency. To compare the hiPSC-derived ECs with mature ECs, we choose HUVECs as control in this study. HUVECs, as mature ECs, displayed contact inhibition and exhibited cobblestone-like morphology. In addition, the HUVECs expressed the specific markers, CD31 and vWF, on membrane and cytoplasm, respectively (supplementary Figures B and C).³⁷

In vivo, the development of human organs/tissues follows a natural development rule. In present study, we explored the possibility to differentiate the hiPSCs based on the principle of vascular system development. Considering the multiple differentiation inducers available and the vascular microenvironment, we proposed a new strategy to differentiate hiPSCs into ECs as shown in Fig. 1(a). On the first day, the hiPSCs were treated with a mixture of specific inducers to initiate mesodermal development and endothelial cell differentiation. As reported, the chemical reagents of BMP4, activin A, FGF-2, and VEGF mediate the commitment of mesoderm to

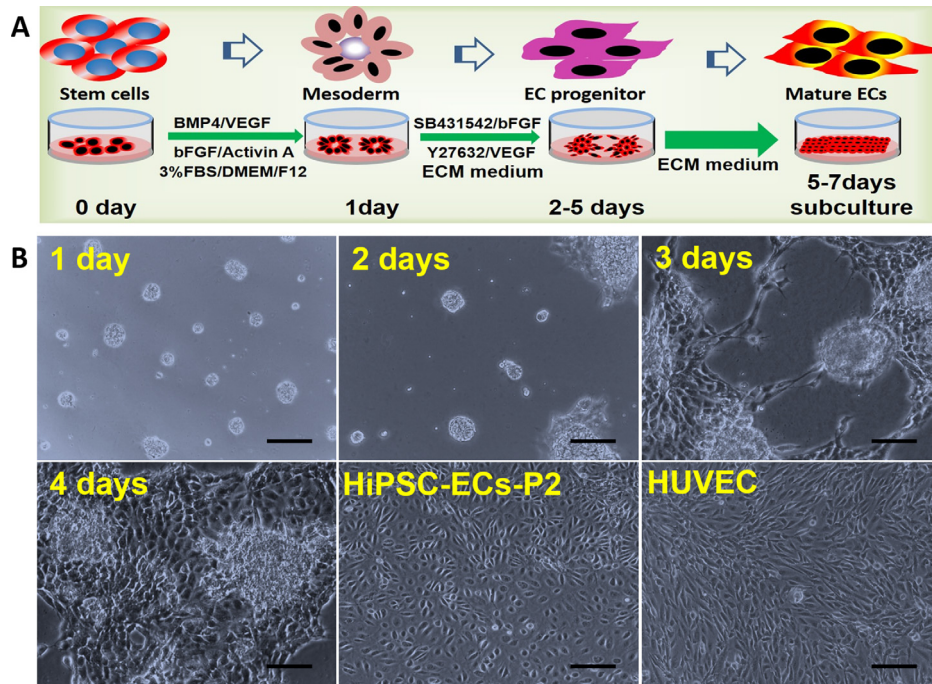


FIG. 1. Differentiation protocol and morphology of hiPSC-ECs. (a) Schematic schedule of the differentiation of hiPSCs into ECs. (b) The hiPSCs formed circular colonies on the first day. Some cells sprouted from the cell aggregates on the second day, and the sprouting branches extended gradually on the third and fourth days. The migrating cells reached 90% confluence on the fifth through seventh days. After scraping away the non-ECs, the cells derived from hiPSCs exhibited cobblestone morphology by passage 2 and appeared similar to HUVECs. P2, passage 2. Scale bar = 100 μm .

differentiate into cardiovascular cells.^{16–20} Y27632, as an inhibitor of rho-associated protein kinase, can inhibit the dissociation-induced apoptosis of human ESCs and enables hESCs to survive in a serum-free medium.²¹ Joo *et al.* found that Y27632 together with VEGF-A strongly promotes the expansion and differentiation of ECs derived from ESCs in a 2-D Matrigel culture system, compared with those incubated with only VEGF-A. They also showed that Y27632 inhibits the differentiation and expansion of mural cells.²² TGF- β -mediated signaling pathways are critical for maintaining vascular homeostasis. SB431542, a selective inhibitor of the TGF- β receptor, promotes the survival of cultured islet ECs by inhibiting apoptosis and maintains their sensitivity to VEGF.²³ Considering the roles of these factors as above, the cultured cells were then treated with Y27632, SB431542, VEGF, and FGF to induce the differentiation, maturation, and proliferation of ECs.

As the composition of serum is complex and variable, a low serum concentration (3%) was used in stage 1 in order to provide the sufficient nutrients required for ECs differentiation and proliferation and to prevent the cells from differentiating into other cell types. As the extracellular microenvironment is crucially important for cell growth, differentiation, and morphogenesis, the extracellular matrix (ECM) was used in stage 2 to promote the proliferation and survival of ECs. *In vitro*, mature vessels with specific functions require the ECM for vascular development and tube formation by ECs, thus, the Matrigel was used as the matrix to provide a suitable microenvironment for the hiPSCs. It is noted, 2-D cell culture is more efficient for differentiating iPSCs into ECs than 3-D culture method. We therefore used a modified 2-D method to mimic the microenvironment required for vessel development.

The dynamic process of endothelial cell differentiation was shown in Fig. 1(b). During stage 1, the hiPSCs formed circles containing around 20 to 50 cells and maintained for 12 to 24 h. Some of these cells migrated from the cellular aggregates on the second day during stage 2. After 3 to 4 days, the sprouting cells formed capillary-like structures. The cells reached 90%

confluence after 4 to 7 days. The confluent cells migrating from the cellular masses exhibited “cobblestone” morphology, which is characteristic of ECs. This process is very similar to culturing ECs derived from animal aortas. When the cells reached confluence, they were subcultured on new Matrigel-coated plates. The P1 cells exhibited typical cobblestone morphology at the edge of the cellular aggregates. The cells in the center were not ECs according to their morphology when they migrated out from the center. When the cells in the center were removed, the P2 cells were contact-inhibited. These findings indicate the feasibility to generate hiPSC-derived endothelial-like cells with maturity property.

B. Genes expression in the process of hiPSCs differentiating into ECs

The organs or tissues can express specific genes and proteins in the different stages during human development. Commonly, the genetic changes are very quicker than that of proteins in this process. Hence, we assessed the relative genes expression of the ECs during the differentiation process in order to reflect the process of vascular development. In this study, the expression of SOX2, a marker of stemness, decreased markedly on the second day (Fig. 2(a)). The level of mRNA encoding brachyury, a specific marker of mesoderm, increased on the second day and then declined rapidly on the fourth day after induction (Fig. 2(b)). These data indicate that the inducers were specific for mesoderm and that the next stage of differentiation occurred quickly and simultaneously.

GATA2 and RUNX1 are transcription factors that regulate the development of the hemogenic endothelium from which hematopoietic and endothelial cells originate.^{20,33,34} The transcription of GATA2 and RUNX1 increased on the second day, indicating early stage vasculogenesis (Figs. 2(c) and 2(d)). The expression of genes encoding VE-cadherin, CD34, and CD31 markers of endothelial progenitor cells and mature ECs increased on the fourth day (Figs. 2(e), 2(f), and 2(h)). Cells of the endothelial lineage and hematopoietic system appear to emerge simultaneously from the mesoderm during embryonic development, because they share a number of transcription factors and surface markers. The expression of the hematopoietic marker SCL mRNA did not increase during differentiation (Fig. 2(g)). These results further demonstrate that the hiPSCs differentiated into ECs. All the gene expression results show that the hiPSCs differentiated into ECs in the course of induction. Furthermore, our differentiation strategy may match the process of vascular development *in vivo* which can intrigue researchers on hematopoietic development.

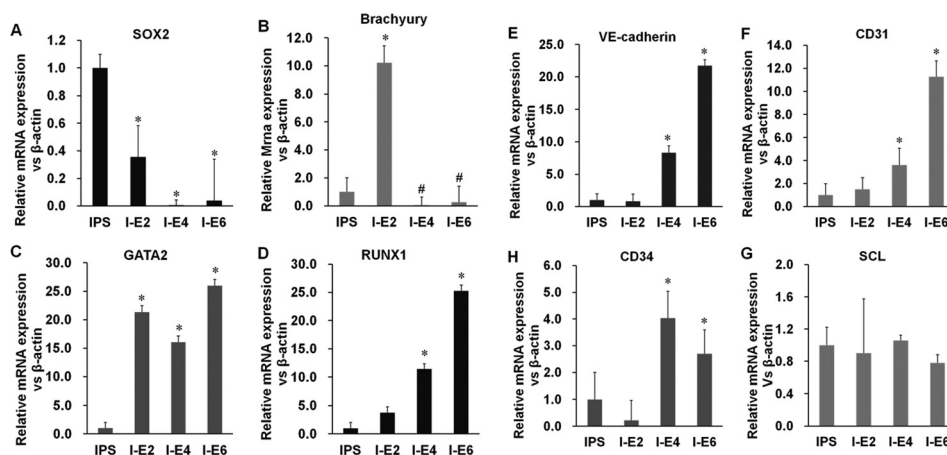


FIG. 2. Gene expression during differentiation. (a) The levels of SOX2 (pluripotency marker) decreased rapidly on the second day of culture. (b) Transcription of the *T* gene encoding brachyury (mesodermal marker) peaked on the second day and then decreased rapidly. (c) and (d) Transcription of the genes encoding the angioblast markers GATA2 and RUNX1 increased after 2 days. (e)–(g) Transcription of the genes encoding VE-cadherin, CD31, and CD34 started to increase on day 4. (h) The level of transcription of *SCL* was unchanged and that of *CD34* increased slightly. I–E(n) = iPSC-ECs (days of differentiation).

C. Expression of functional proteins in hiPSC-derived ECs

The mature endothelial cells express marker proteins and possess specific functions which distinguish ECs from other cells. CD31 and vWF are well known as ECs marker proteins. In this study, we analyzed the CD31 and vWF expression of hiPSC-derived ECs by immunofluorescence assays. The results indicated that CD31 was expressed in the cellular membrane and vWF was expressed in the cytoplasm (Fig. 3(a)). This is very similar to the expression seen in HUVECs, which served as the positive control (supplementary Figure B).³⁷

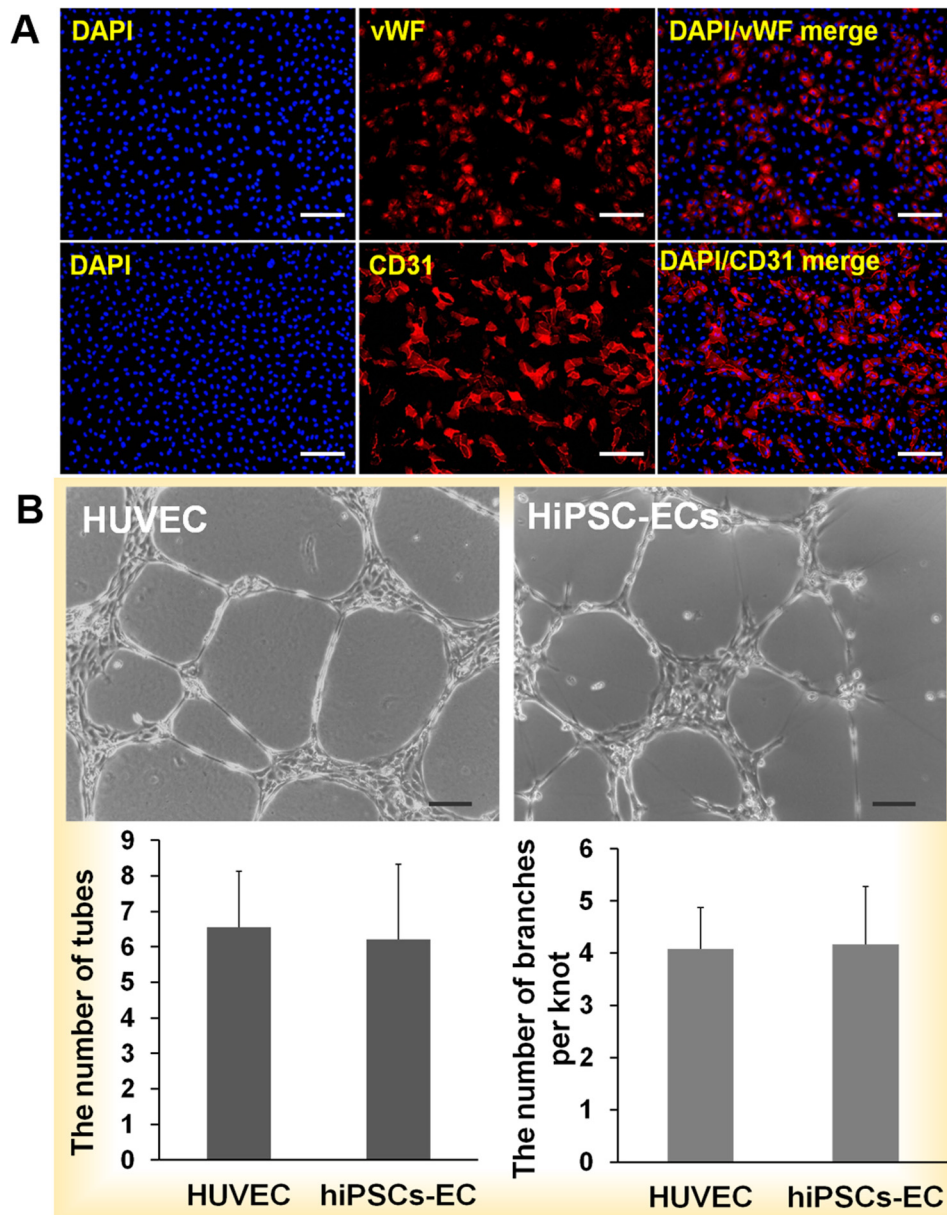


FIG. 3. Identification of hiPSC-derived ECs and tube formation. (a) Immunofluorescence analysis of CD31 and vWF expression by hiPSC-derived ECs. Most of the cells derived from hiPSCs expressed the endothelial cell-specific markers CD31 on membranes and vWF in the cytoplasm. HUVECs expressed CD31 on the outer membrane. The nuclei were counterstained with DAPI. (b) hiPSC-ECs-P1 and HUVECs-P1 were cultured on Matrigel for 24 h, and sprouting cells formed a network among the cellular aggregates. The numbers of complete tubes and branches per knot were similar to those of HUVECs. Scale bar = 100 μ m.

Mature ECs have the ability to form tubes on the thick Matrigel. To evaluate the functioning of the hiPSC-derived ECs, P1 cells were evaluated for their ability to form tubes. The capillary networks of HUVECs and hiPSC-derived ECs were observed after 24 h (Fig. 3(b)). We call one cellular mass a knot that sprouts, and the sprouting cells are called branches. There was no significant difference in the numbers of complete tubes or branches per knot in cultures of HUVECs and hiPSC-derived ECs (Fig. 3(b)), indicating that the ECs derived from hiPSCs functioned similarly to mature HUVECs. Mature ECs are very important for research into vascular disease such as inflammation and atherosclerosis. In addition, mature ECs are essential for functional engineered tissues or organs. Obtaining individual ECs to construct specific organs is the best approach.

D. Assessment of purity of hiPSC-derived ECs

The differentiation efficiency of ECs from hiPSCs in the published methods is still very low. To assess our differentiation strategy, we used flow cytometry to evaluate the purity of the mature hiPSC-derived ECs. CD31 protein is known as one of marker of vascular endothelial cells. Thus, we determined the number of P1 cells that expressed the endothelial cell marker CD31. The cells were manually separated from non-ECs. More than 60% of the hiPSC-derived ECs were CD31-positive (Fig. 4). The results demonstrate that our differentiation efficiency is greater than that achieved by previous methods. Although the purity of the hiPSC-ECs does not meet the demands of basic research and cellular therapy, more ECs can be obtained via sorting

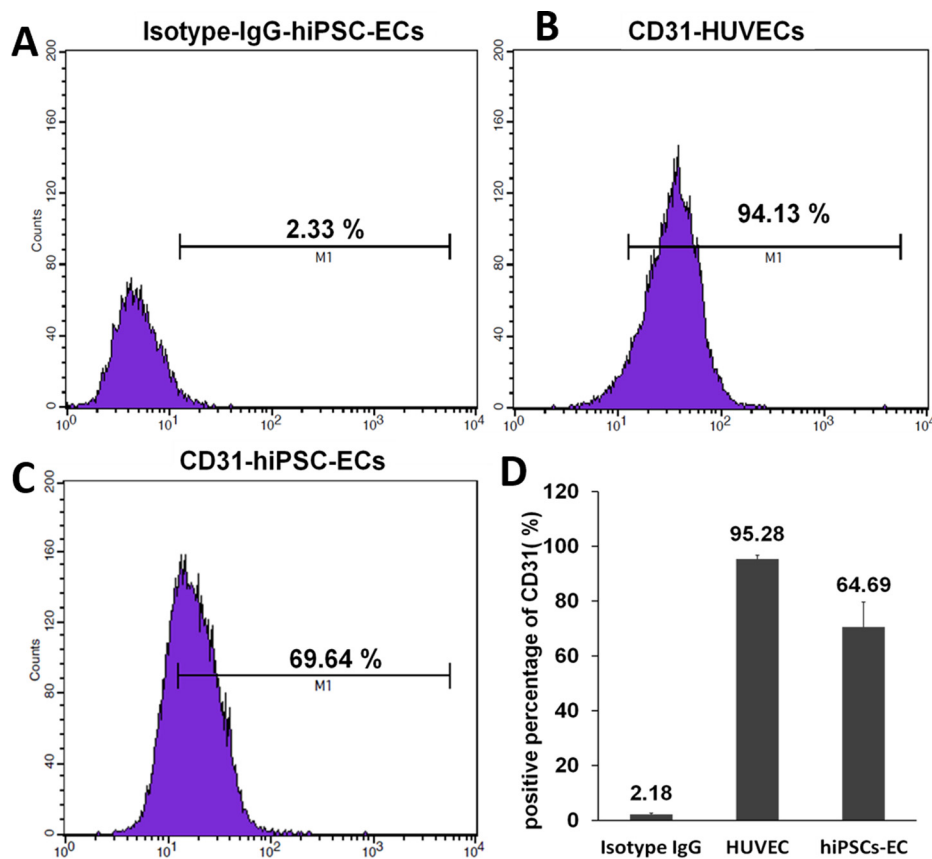


FIG. 4. Flow cytometric analysis of CD31 expression by hiPSC-ECs. (a) Detection using an IgG isotype matched antibody (negative control). (b) Over 90% HUVECs were CD31-positive. (c) Over 60% hiPSC-ECs were CD31-positive. (d) The average number of CD31-positive cells was calculated for three independent experiments. The average values are shown above the columns.

technology using our methods, suggesting it has potential for applications in vascular engineering.

E. hiPSC-derived ECs in response to low flow stress

Normal blood vessels can respond to blood stream stress under physiological conditions. ECs reside in the vascular lumen and are directly exposed to flowing blood. This flow can influence the arrangement of ECs. In this study, the ECs are exposed to a low flow rate at 10 dyn/cm^2 on a microfluidic device, mimicking the physiological level of flow stimulation within small or microvessels *in vivo*.^{27,28} The design and fabrication of the microfluidic device are shown in Figs. 5(a) and 5(b). The hiPSCs derived ECs seeded in the microchannels and the hiPSC-ECs exhibited strong expression of CD31 protein after MACS purification. After the ECs were seeded in the microchannels, they could grow well in the microchannels over three days and then were exposed to physiological flow at 10 dyn/cm^2 for 24 h. The cells were then analyzed by immunofluorescence assay using CD31 antibodies as shown in Fig. 6. The number of cells in flow condition with the direction of long axis at range of -30° to $+30^\circ$ are more than static condition. The results demonstrated an ordered arrangement in cells morphology under flow condition as compared to static condition. The long axis of most hiPSC-ECs and the distribution of membrane protein CD31 on ECs were arranged following the flow direction. However, the ECs displayed a disordered arrangement in static condition, indicating the functional response of ECs to the physiological level of flow. Obviously, the established system can be further used to study the mechanism of ECs physiology and patho-physiology in different diseases.

F. Response of hiPSC-derived ECs to inflammatory stimulation under flow condition

Generally, ECs can react to inflammatory factors or inflammatory cells in blood vessels in pathological process. To mimic the inflammatory response of hiPSC-derived ECs under external stimulation, we conducted the microfluidic-based cellular assay as shown in Fig. 5(c). The hiPSC-derived ECs were cultured in the microchannels as described above. The cells were treated with $\text{TNF-}\alpha$, a well known inducer of vascular inflammation *in vivo* and *in vitro*.^{35,36} under the low flow rate at 1 dyn/cm^2 . The control group was treated with normal medium at same flow rate. This flow rate is significantly lower than that of physiological level flow

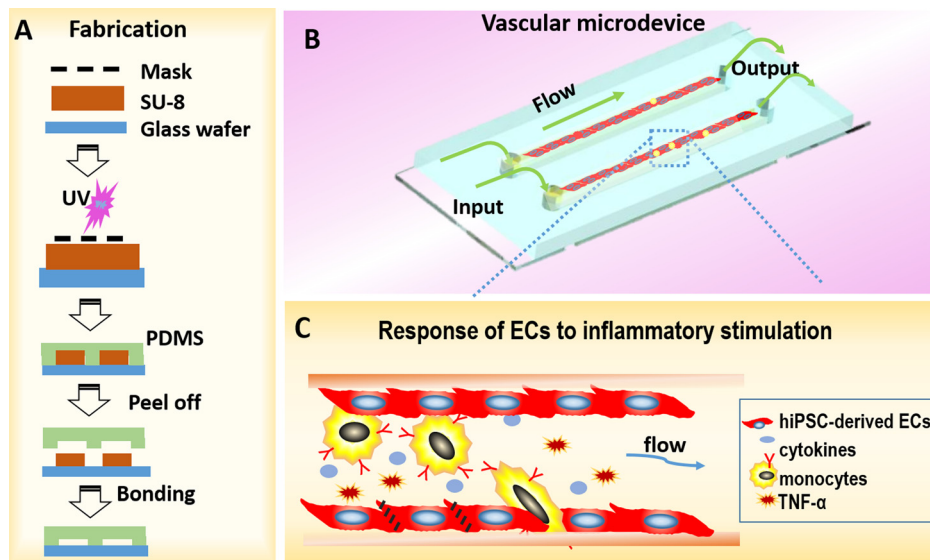


FIG. 5. Schematic of microdevice and vascular inflammation. (a) The procedure of fabricating microdevice. (b) The schematic diagram of vascular inflammation on chip. The microdevice has three parts: a glass substrate layer, a layer of polydimethylsiloxane (PDMS) with channels, and a perfusion system. (c) The enlarged view of red frame in B represents the interaction between inflammatory cells and endothelial cells.

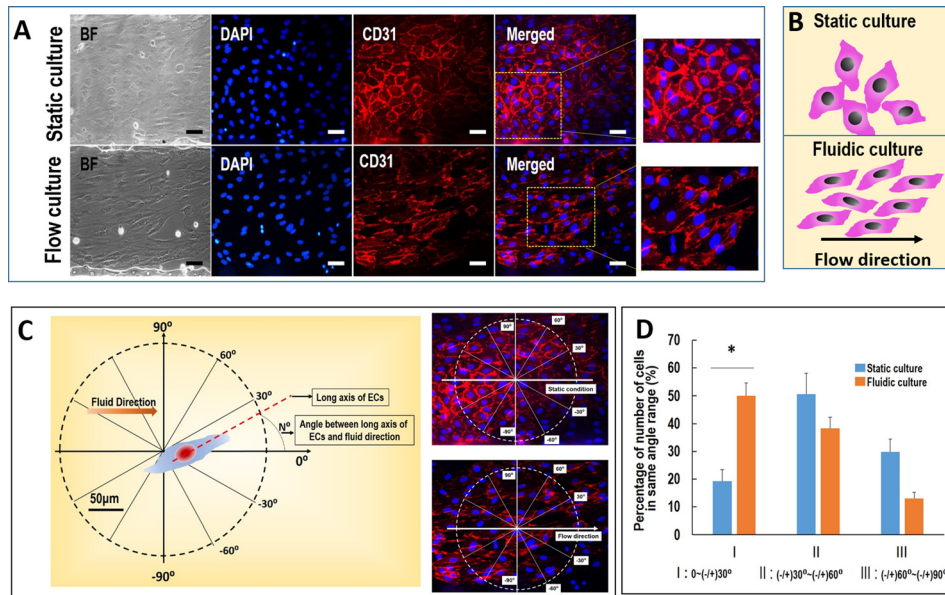


FIG. 6. The effects of flow stress on the arrangement of hiPSC-ECs. (a) Immunofluorescence assay showing the morphology of hiPSC-ECs under physiological relevant flow stress using CD31 antibodies. The nuclei were counterstained with DAPI. (b) The schematic diagram of the arrangement of hiPSC-ECs under static culture and flow culture. The hiPSC-ECs aligned with flow direction. (c) and (d) The arrangement of hiPSC-ECs under flow stress. The cellular arrangement was defined as the angle between the cellular long axis and the flow direction. The number of cells within same angle area in unit circle area was counted according to the cell arrangement. The angular range was divided as -30° to $+30^\circ$, 30° to 60° / -30° to -60° , 60° to 90° / -60° to -90° . BF: bright field. Scale bar = $50 \mu\text{m}$.

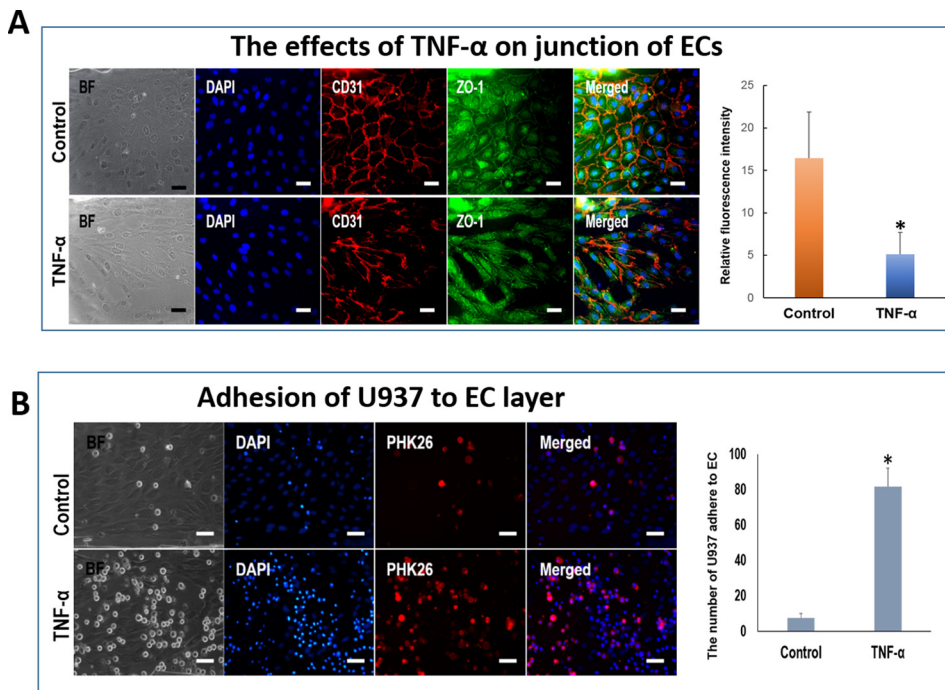


FIG. 7. Interaction between U937 cells and hiPSC-ECs under inflammation. (a) The hiPSC-ECs in microchannels were treated with TNF- α under low flow stress. The membrane protein CD31 and tight junction protein ZO-1 were stained by immunofluorescence assay. The nuclei were counterstained with DAPI. The histogram indicates the relative fluorescence intensity of ZO-1. (b) U937 cells adhering to the hiPSC-ECs in microchannels under inflammation conditions treated with TNF- α . Normal medium was used as the control. Right figure indicates that number of U937 cells adhering to the ECs. BF: bright field. Scale bar = $50 \mu\text{m}$.

because the presence of lower flow in inflammatory vessels. Even, seriously inflammatory response can induce stagnation of blood in part of vessels segment. Blood stasis can promote inflammatory cells to adhere to and migrate across endothelium. When blood vessels initiate inflammation, the junction of endothelial was damaged, which promoted the inflammatory cells migrating into perivascular tissues in the process of vascular inflammation.

As shown in Fig. 7(a), the junctions of ECs disrupted significantly after the addition of TNF- α under flow condition. The cells exhibited weak expression of tight junction protein, ZO-1 with discontinued cell junctions. The results indicated that the tight junction of ECs was damaged by the TNF- α . In addition, to explore the adhesion ability of the damaged ECs to inflammatory monocyte, we introduced the suspension of human monocytic tumor cells, U937 cells to the microchannels seeded with ECs. The results demonstrated a higher percentage of adhesive monocytes on the ECs pretreated with TNF- α than that of ECs alone (Fig. 7(b)). These results demonstrated that TNF- α can damage the tight junction of hiPSC-derived ECs or promote adhesion molecules expression of ECs, which might lead to the adhesion of inflammatory cells to the ECs. Further work is needed to investigate the adhesion mechanism of the hiPSCs derived ECs exposed to inflammatory factors or external stimulations in vascular-related diseases.

V. CONCLUSIONS

In this study, we present a new and efficient strategy to differentiate hiPSCs into endothelial cells within short time and effectively mimic the inflammatory response of endothelial cells under physiological relevant flow. We explored the feasibility to combine the necessary inducers to maintain proper differentiating microenvironment following inducing vascular development principle. The hiPSC-derived endothelial cells exhibit the essential properties of mature ECs, including the expression of cells-specific genes and proteins and tube formation ability. Moreover, hiPSC-derived ECs can respond to inflammatory stimulation in the presence of monocytes under flow condition, indicating the utility of the hiPSC-derived ECs for the creation of vascular organ-on-a-chip, and the study of vascular pathologies in different diseases and tissue engineering applications.

ACKNOWLEDGMENTS

This work was supported by the Major International Cooperation Program (81220108002 to S. Chen), Key Programs (30830050 to S. Chen and 81130004 to A. F. Chen), Great Research Plan Project (91539120 to S. Chen), and General Programs (81170298 and 81270410 to D. Meng, 81100047 and 81470260 to M. Xiang, and 81201468 to X. H. Wang) of the National Natural Science Foundation of China as well as the Key Laboratory of Separation Sciences for Analytical Chemistry, Dalian Institute of Chemical Physics, and by the International Sciences & Technology Cooperation Program of China (2015DFA00740) and National Nature Science Foundation of China (Nos. 31171149 and 91543121).

¹P. Carmeliet, *Nature* **438**, 932–936 (2005).

²K. H. Park and W. J. Park, *J. Korean Med. Sci.* **30**, 1213–1225 (2015).

³U. K. Sampson, M. M. Engelgau, E. K. Peprah, and G. A. Mensah, *Cardiovasc. J. Afr.* **26**, S56–S60 (2015).

⁴M. M. Polovina and T. S. Potpara, *Postgrad. Med.* **126**, 38–53 (2014).

⁵K. Takahashi and S. Yamanaka, *Cell* **126**, 663–676 (2006).

⁶K. Takahashi, K. Tanabe, M. Ohnuki, M. Narita, T. Ichisaka, K. Tomoda, and S. Yamanaka, *Cell* **131**, 861–872 (2007).

⁷J. Yu, M. A. Vodyanik, K. Smuga-Otto, J. Antosiewicz-Bourget, J. L. Frane, S. Tian, J. Nie, G. A. Jonsdottir, V. Ruotti, R. Stewart, I. I. Slukvin, and J. A. Thomson, *Science* **318**, 1917–1920 (2007).

⁸S. Kusuma, Y. I. Shen, D. Hanjaya-Putra, P. Mali, L. Cheng, and S. Gerech, *Proc. Natl. Acad. Sci. U. S. A.* **110**, 12601–12606 (2013).

⁹S. C. Desbordes and L. Studer, *Nat. Protoc.* **8**, 111–130 (2013).

¹⁰M. Serra, C. Brito, C. Correia, and P. M. Alves, *Trends Biotechnol.* **30**, 350–359 (2012).

¹¹M. Fujiwara, P. Yan, T. G. Otsuji, G. Narazaki, H. Uosaki, H. Fukushima, K. Kuwahara, M. Harada, H. Matsuda, S. Matsuoka, K. Okita, K. Takahashi, M. Nakagawa, T. Ikeda, R. Sakata, C. L. Mummery, N. Nakatsuji, S. Yamanaka, K. Nakao, and J. K. Yamashita, *PLoS One* **6**, e16734 (2011).

¹²Z. Alipio, W. Liao, E. J. Roemer, M. Waner, L. M. Fink, D. C. Ward, and Y. Ma, *Proc. Natl. Acad. Sci. U. S. A.* **107**, 13426–13431 (2010).

- ¹³A. J. Rufaihah, N. F. Huang, S. Jamé, J. C. Lee, H. N. Nguyen, B. Byers, A. De, J. Okogbaa, M. Rollins, R. Reijo-Pera, S. S. Gambhir, and J. P. Cooke, *Arterioscler., Thromb., Vasc. Biol.* **31**, e72–e79 (2011).
- ¹⁴N. M. Kane, M. Meloni, H. L. Spencer, M. A. Craig, R. Strehl, G. Milligan, M. D. Houslay, J. C. Mountford, C. Emanuelli, and A. H. Baker, *Arterioscler., Thromb., Vasc. Biol.* **30**, 1389–1397 (2010).
- ¹⁵S. Zhang, J. R. Dutton, L. Su, J. Zhang, and L. Ye, *Biomaterials* **35**, 3786–3793 (2014).
- ¹⁶D. Evseenko, Y. Zhu, K. Schenke-Layland, J. Kuo, B. Latour, S. Ge, J. Scholes, G. Dravid, X. Li, W. R. MacLellan, and G. M. Crooks, *Proc. Natl. Acad. Sci. U. S. A.* **107**, 13742–13747 (2010).
- ¹⁷S. Pearson, P. Sroczynska, G. Lacaud, and V. Kouskoff, *Development* **135**, 1525–1535 (2008).
- ¹⁸O. Goldman, O. Feraud, J. Boyer-Di Ponio, C. Driancourt, D. Clay, M. C. Le Bousse-Kerdiles, A. Bennaceur-Griscelli, and G. Uzan, *Stem Cells* **27**, 1750–1759 (2009).
- ¹⁹F. Lanner, M. Sohl, and F. Farnébo, *Arterioscler., Thromb., Vasc. Biol.* **27**, 487–493 (2007).
- ²⁰M. J. Karkkainen, P. Haiko, K. Sainio, J. Partanen, J. Taipale, T. V. Petrova, M. Jeltsch, D. G. Jackson, M. Talikka, H. Rauvala, C. Betsholtz, and K. Alitalo, *Nat. Immunol.* **5**, 74–80 (2004).
- ²¹A. Honda, M. Hirose, and A. Ogura, *Exp. Cell Res.* **315**, 2033–2042 (2009).
- ²²H. J. Joo, D. K. Choi, J. S. Lim, J. S. Park, S. H. Lee, S. Song, J. H. Shin, D. S. Lim, I. Kim, K. C. Hwang, and G. Y. Koh, *Blood* **120**, 2733–2744 (2012).
- ²³C. E. Clarkin, A. J. King, P. Dhadda, P. Chagastelles, N. Nardi, C. P. Wheeler-Jones, and P. M. Jones, *Stem Cells* **31**, 547–559 (2013).
- ²⁴N. Sun, N. J. Panetta, D. M. Gupta, K. D. Wilson, A. Lee, F. Jia, S. Hu, A. M. Cherry, R. C. Robbins, M. T. Longaker, and J. C. Wu, *Proc. Natl. Acad. Sci. U. S. A.* **106**, 15720–15725 (2009).
- ²⁵H. Wen, X. Gao, and J. Qin, *Integr. Biol. (Cambridge)* **6**, 35–43 (2014).
- ²⁶L. Wang, S. Tang, Y. Wang, S. Xu, J. Yu, X. Zhi, Z. Ou, J. Yang, P. Zhou, and Z. Shao, *Clin. Exp. Metastasis* **30**, 671–680 (2013).
- ²⁷C. Cheng, F. Helderman, D. Tempel, D. Segers, B. Hierck, R. Poelmann, A. van Tol, D. J. Duncker, D. Robbers-Visser, N. T. Ursem, R. van Haperen, J. J. Wentzel, F. Gijsen, A. F. van der Steen, R. de Crom, and R. Krams, *Atherosclerosis* **195**(2), 225–235 (2007).
- ²⁸M. Raasch, K. Rennert, T. Jahn, S. Peters, T. Henkel, O. Huber, I. Schulz, H. Becker, S. Lorkowski, H. Funke, and A. Mosig, *Biofabrication* **7**(1), 015013 (2015).
- ²⁹M. Dick, K. MacDonald, J. C. Tardif, and R. L. Leask, *Biomed. Eng. Online* **14**, 58 (2015).
- ³⁰J. J. Chiu, L. J. Chen, C. N. Chen, P. L. Lee, and C. I. Lee, *J. Biomech.* **37**, 531–539 (2004).
- ³¹E. W. Young and C. A. Simmons, *Lab Chip* **10**, 143–160 (2010).
- ³²M. Rossi, R. Lindken, B. P. Hierck, and J. Westerweel, *Lab Chip* **9**, 1403–1411 (2009).
- ³³J. J. Lugus, Y. S. Chung, J. C. Mills, S. I. Kim, J. Grass, M. Kyba, J. M. Doherty, E. H. Bresnick, and K. Choi, *Development* **134**, 393–405 (2007).
- ³⁴E. de Pater, P. Kaimakis, C. S. Vink, T. Yokomizo, T. Yamada-Inagawa, R. van der Linden, P. S. Kartalaei, S. A. Camper, N. Speck, and E. Dzierzak, *J. Exp. Med.* **210**, 2843–2850 (2013).
- ³⁵M. W. Kang, H. J. Song, S. K. Kang, Y. Kim, S. B. Jung, S. Jee, J. Y. Moon, K. S. Suh, S. D. Lee, B. H. Jeon, and C. S. Kim, *Korean J. Physiol. Pharmacol.* **19**, 229–234 (2015).
- ³⁶J. DeSousa, M. Tong, J. Wei, L. Chamley, P. Stone, and Q. Chen, “The anti-inflammatory effect of calcium for preventing endothelial cell activation in preeclampsia,” *J. Hum. Hypertens.* (published online 2015).
- ³⁷See supplementary material at <http://dx.doi.org/10.1063/1.4940041> for immunofluorescence analysis of hiPSCs and HUVECs and the primer sequences.